DTU Library

Comparison of effective noise temperatures in YBa2BCu3O7- junctions

Fischer, Gerd Michael; Mygind, Jesper; Pedersen, Niels Falsig

Published in:
I E E E Transactions on Applied Superconductivity

Link to article, DOI:
10.1109/77.622210

Publication date:
1997

Document Version
Publisher's PDF, also known as Version of record

Comparison of Effective Noise Temperatures in $YBa_2Cu_3O_{7-\delta}$ Junctions

Gerd M. Fischer, Jesper Mygind, and Niels F. Pedersen
Department of Physics, Technical University of Denmark, DK-2800 Lyngby, Denmark

***Abstract*—The dc voltage response to 70 GHz radiation was measured for YBCO bicrystal junctions, step edge junctions and ramp edge junctions at temperatures from 4 K to 90 K. Employing the RSJ-model and assuming thermal noise, the Josephson radiation is about equal to the voltage difference of the voltage response to the small signal microwave irradiation. In the presence of excess noise, an effective noise temperature can be defined and is used as a figure of merit. In bicrystal grain boundary junctions with zero magnetic field the effective noise temperature was determined to be equal to the physical temperature within experimental error. Bicrystal grain boundary junctions with non-zero magnetic field, step edge junctions and ramp edge junctions showed excess noise. The scaling of the noise temperature is compared with the width of the junction in units of the Josephson penetration depth.**

I. Introduction

The large energy gap of the high-T_c superconductors opens the possibility for high frequency applications and for higher operating temperatures of electronic circuits and devices. The high frequency performance can be determined measuring the linewidth of the Josephson radiation. Comparing the noise temperature deduced from the linewidth with the physical temperature will determine the presence of excess noise. The noise temperature of the single junction will be used as a figure of merit.

In this paper a comparison of the results obtained on $YBa_2Cu_3O_{7-\delta}$ bicrystal grain boundary junctions, step edge grain boundary junctions and ramp edge junctions is presented.

II. Theoretical Background

Employing the Resistively Shunted Junction (RSJ) model, thermal noise will lead to a Josephson oscillation linewidth (FWHM) [1],

$$\Delta\nu = 4\pi \cdot \left(\frac{2e}{h}\right)^2 \cdot R_d^2 \cdot \frac{k_B T}{R_n} \cdot \left(1 + \frac{I_c^2}{2I_{dc}^2}\right) \qquad (1)$$

Here, I_c denotes the critical current, R_n the normal state resistance, I_{dc} the bias current and R_d the differential resistance at $V \cong h/2e\ \nu$, where ν is the frequency of the

Manuscript received August 27, 1996.

G. M. Fischer, present address: Physics Department, Chalmers University of Technology and Gothenburg University, S-41296 Gothenburg, Sweden, phone +46-31-772-3319, fax: +46-31-772-3471, gmf@fy.chalmers.se, http://fy.chalmers.se/~gmf.

This work was supported in parts by the European Union ESPRIT Basic Research project 7100.

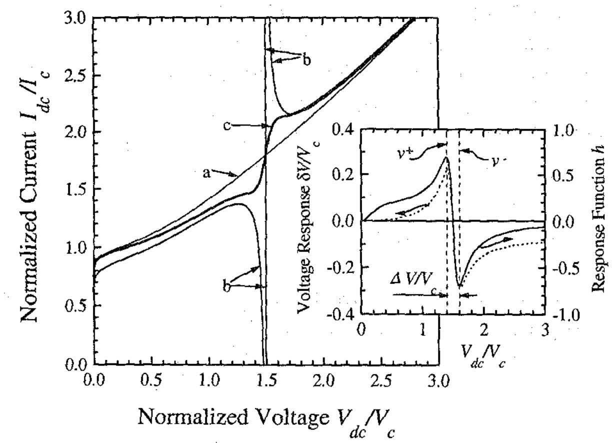

Figure 1. Response of an RSJ model junction to external microwave irradiation at frequency $\nu/\nu_c = 1.5$, with $\nu = 2e/h\ V$, $\nu_c = 2e/h\ V_c$ and $V_c = I_c R_n$. The IVc is shown for the autonomous junction (a), the irradiated junction without noise (b) and with noise (c). To avoid the response singularity for $\nu \cong 0$, a noise rounding of the critical current with $(2e/h)\, I_c/(2\pi k_B T) = 100$ was used. The change in the IVc is amplified by an artificially large microwave current ($I_{rf} = I_c$) for clear presentation. For case (b), the wideband response for $V < h/2e \cdot \nu$ and the selective response with the singularity at $V \cong h/2e \cdot \nu$ is seen. In case (c) the singularity is removed due to the finite linewidth $\Delta\nu = 0.2\ \nu_c$. The inset shows the voltage response $\delta V/V_c$ and the response function $h(\nu) = 8/\pi \cdot I/I_c \cdot V/V_c \cdot \Delta I/I_c$. The voltage difference $\Delta V/V_c = \nu^- - \nu^+$ between the response voltage extrema at ν^+ and ν^- is about equal to the linewidth $\Delta\nu \cong 2e/h\ \Delta V$.

applied *rf* signal. Assuming thermal noise the linewidth has a Lorentzian shape with FWHM of $\Delta\nu$. In the presence of additional noise sources, it is convenient to define an effective noise temperature, T_{eff}, [1] with

$$T_{eff} = \Delta\nu \cdot \frac{1}{4\pi} \cdot \left[\left(\frac{2e}{h}\right)^2 \cdot R_d^2 \cdot \frac{k_B}{R_n} \cdot \left(1 + \frac{I_c^2}{2I_{dc}^2}\right)\right]^{-1}$$

After determining $\Delta\nu$, R_d, R_n, I_{dc}, and I_c experimentally, the effective noise temperature can be calculated. Rigorously the derivation holds for small junctions with white noise spectrum, at high temperatures in the zero capacitance limit, where the RSJ model applies. In lack of a theoretical description of the Josephson linewidth for large overdamped Josephson junctions, we will use this derivation for those as well. R_d, R_n, I_{dc}, and I_c can be determined from the *dc IV* curve. The linewidth of the Josephson radiation, $\Delta\nu^{jct}$, can either be obtained by direct measurement with a superheterodyne receiver, or using the detector response of the Josephson junction to irradiation at frequency ν. For the latter case, in the small signal limit and the small linewidth limit, $\Delta\nu << \nu$, the linewidth, $\Delta\nu$, is about equal to the

1051-8223/97$10.00

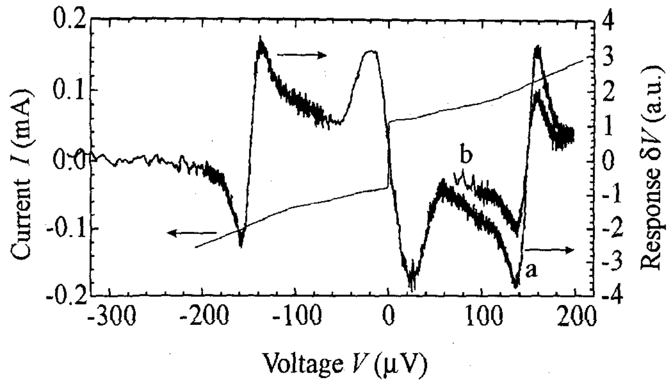

Figure 2. *IV* curve and voltage response of junction Y-EG6-4 at T≈45 K under 70 GHz irradiation. The response is shown for two power levels differing by 3 dB. In the small signal limit the pumped and the unpumped *IV* curves are indistinguishable.

difference in the bias voltage, $\Delta V/V_c = \nu^{-}-\nu^{+}$, of the extrema of the voltage response, δV. Using the *ac* Josephson relation $\Delta\nu \cong 2e/h\, \Delta V$. If the junction linewidth, $\Delta\nu^{jct}$, is smaller than the external linewidth, $\Delta\nu^{ext}$, then $\Delta\nu^{jct}$ can be extracted using a Hilbert transformation of the response function h [2,3]. In the opposite case, applicable to the measurements presented here, the linewidth $\Delta\nu^{jct}$ differs from the voltage difference ΔV by less than two percent for frequencies up to $3\nu_c$ [4], where $\nu_c = 2e/h\, I_c R_n$.

III. Experimental Techniques

Practically, the direct measurement of the Josephson linewidth is limited to low noise junctions with low differential resistance on low loss substrates. For junctions on high loss substrates like $SrTiO_3$ the linewidth of the Josephson radiation can be deduced from the small signal response of the junction to high frequency irradiation.

The samples were mounted in a vacuum can and immersed in a double μ-metall screened cryostat. *Dc* connections for four point measurements were supplied and the sample placed across the open end of a 70 GHz hollow wave guide providing loose *rf* coupling. The temperature was monitored with a Si diode thermometer. All the measurements were carried out in an *rf* shielded room. The samples were irradiated using a 70 GHz Gunn diode with a radiation linewidth (FWHM) $\Delta\nu^{ext} < 10$ kHz. The power could be adjusted with a high precision attenuator.

The *rf* signal was modulated using an *rf* off/on switch and the response was extracted employing a lock-in technique. A small coil enabled the application of a small magnetic field perpendicular to the substrate plane. Fig. 2 shows the *IV* curve of a particular junction (Y-EG6-4) and the voltage response, δV, to high frequency irradiation with ν = 70 GHz. For positive bias, δV is shown for two microwave power levels differing by 3 dB. In the small signal limit, the difference, ΔV, of bias voltage at the response extrema is independent of the applied power.

IV. Samples

The measurements were performed on $YBa_2Cu_3O_{7-\delta}$ Josephson junctions on $SrTiO_3$ bicrystal substrates prepared at NKT Research Center (NKT), and the University of Tübingen (Y-EG), step edge junctions on $LaAlO_3$ from the Forschungszentrum Jülich (SEJ) and ramp edge junctions (LEJ) from IBM Research Laboratories, Yorktown Heights.

The NKT samples were prepared by pulsed laser deposition (PLD) of a 330 nm thick $YBa_2Cu_3O_{7-\delta}$ layer on a symmetric 24° misorientation angle bicrystal $SrTiO_3$ substrate. Microbridges with widths from 2 to 48 μm were patterned using e-beam lithography and Ar ion milling [5]. The Tübingen samples (Y-EG) were prepared on similar substrates by dc magnetron sputtering and patterned to microbridges of 5 to 20 μm width with optical lithography and Ar ion milling [6]. For the step edge junctions (SEJ) first a step of 120 nm height and 80° angle was etched into the substrate. Then the substrate was covered with a $YBa_2Cu_3O_{7-\delta}$ thin film by PLD and microbridges of width 16 and 32 μm patterned by optical lithography and Ar ion milling [7]. The ramp edge junctions (LEJ) were fabricated in a three step process [8]. After depositing a 300 nm $YBa_2Cu_3O_{7-\delta}$ base layer, and a 500 nm insulating MgO layer through a stencil mask, the base layer was patterned with Ar ion milling. Prior to the deposition of the MgO barrier of roughly 2 nm by *rf* sputtering, an in-situ ion milling was performed to clean the junction surface. The $YBa_2Cu_3O_{7-\delta}$ counterelectrode and Ag contact pads were then deposited. Patterning with photoresist and ion milling completed the fabrication of the devices with widths between 5 μm and 20 μm.

V. Experimental Results

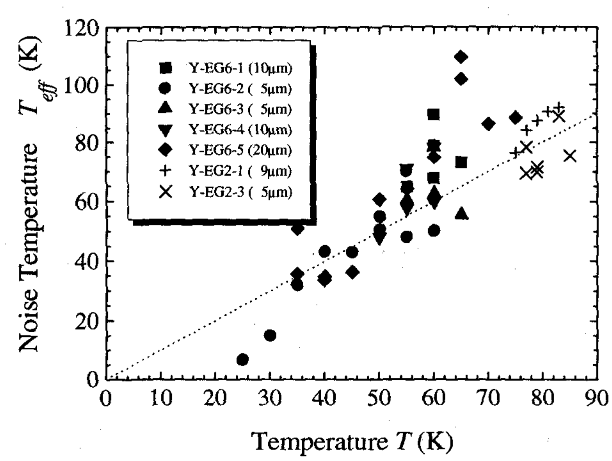

Figure 3. Noise temperature T_{eff} versus physical temperature T for the bicrystal junctions Y-EG. The data points were obtained with an applied magnetic field to maximize the critical current with bias polarity, case *max* I_c^+ (for details see text).

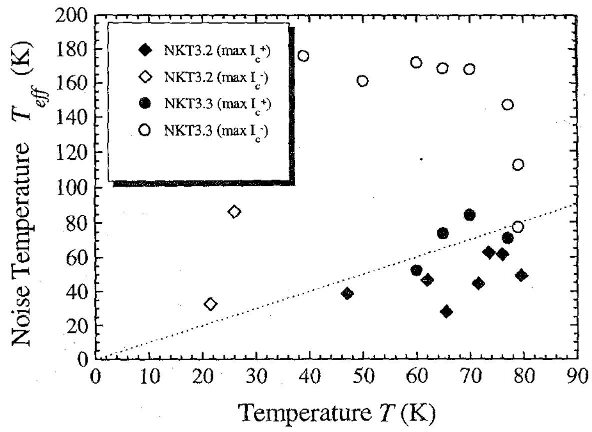

Figure 4. Noise temperature T_{eff} versus physical temperature T for bicrystal junctions NKT3.2 and NKT3.3. Measurements were taken with an applied magnetic field to maximize the critical current with bias polarity (closed symbols), *max* I_c^+, and opposite to bias polarity (open symbols), *max* I_c^-.

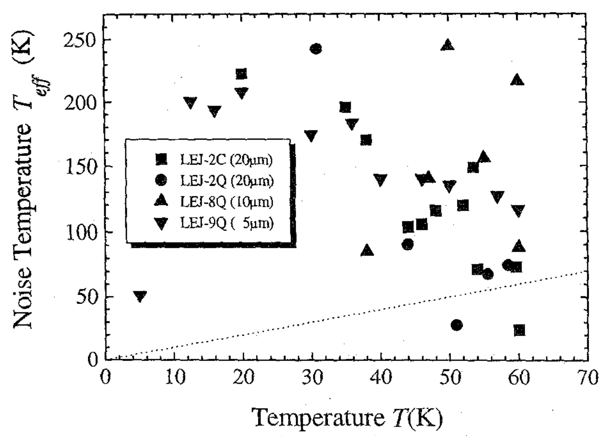

Figure 6. Noise temperature T_{eff} versus physical temperature T for the ramp edge junctions LEJ. The data points were obtained with an applied magnetic field used to maximize the critical current with bias polarity, *max* I_c^+.

A. Bicrystal junctions Y-EG

In Fig. 3 the effective noise temperature, T_{eff}, of the junctions on chip Y-EG2 and Y-EG6 is plotted versus the physical temperature, T. The noise temperatures are within the experimental error equal to the physical temperature.

B. Bicrystal junctions NKT

Due to the large I_cR_n product, the junctions exhibited a very large resistance at $V = 145\,\mu$V, corresponding to 70 GHz. Under the condition of a maximized critical current (*max* I_c^+), using a small applied magnetic field, the linewidth of the Josephson radiation could only be measured for the three smaller junctions and above 30 K. For these measurements, the noise temperature T_{eff} is equal to the physical temperature T within experimental error [6].

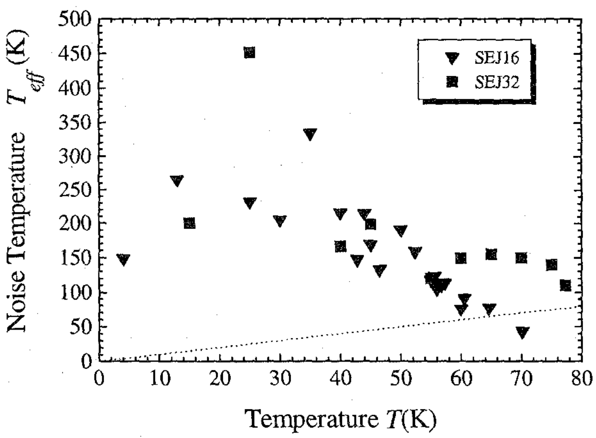

Figure 5. Noise temperature T_{eff} versus physical temperature T for the step edge junctions SEJ. The data points were obtained with an applied magnetic field used to maximize the critical current with bias polarity, *max* I_c^+ (for details see text).

With a large differential resistance R_d, the linewidth $\Delta\nu^{jct}$ is larger than the applied frequency ν and the selective response is not detectable. This was the case for the larger junctions at intermediate and low temperatures, and for some of the smaller junctions at low temperatures. Thus, an applied magnetic field was used to maximize the critical current of the opposite polarity, i.e. to maximize the negative critical current value when measuring the selective response at the positive bias current (*max* I_c^-). Since the junctions exhibit an $I_c(V,H)$ dependence similar to a junction with asymmetrical inline/overlap geometry [9,10], such an applied magnetic field leads to a decrease of the critical current of the bias current polarity and to a reduced differential resistance in the bias point. The smaller differential resistance transforms the current noise to a smaller value of voltage noise. This reduces the linewidth, and the selective response is measurable. Fig. 4 shows the noise temperatures for the junction NKT3.2 and NKT3.3 in the two different regimes, *max* I_c^+ and *max* I_c^-. The data points obtained for *max* I_c^+ (closed symbols) are close to the $T_{eff}/T = 1$ (dotted line). Maximizing the critical current of opposite polarity (open symbols), *max* I_c^-, the noise temperature increases up to a factor of 4 for these junctions. The noise temperature is increased for the majority of the measurements in this regime. Especially, in the intermediate temperature range T_{eff} as high as $1.6{\cdot}10^3$ K has been observed [6].

C. Step edge junctions SEJ

Only at temperatures close to T_c, T_{eff} approaches the physical temperature T. Decreasing T increases the noise temperature with a maximum in the intermediate temperature range (see Fig. 5). The noise temperature resembles the dependence observed for the sample NKT for the case *max* I_c^-. In contrast to those measurements, here the applied magnetic field always was chosen to maximize the critical current of the same polarity as the bias current (*max* I_c^+).

The effective noise temperature T_{eff} could not be reduced by adjusting the magnetic field. Even for junctions with widths smaller than 4 λ_J, T_{eff} is considerably larger than the physical temperature T (see Fig. 7).

D. Ramp edge junctions LEJ

Below 50 K some junctions showed flux flow behavior, above 50 K all RSJ like *IVc*'s. Only measurements with RSJ characteristics were used. Again, a small magnetic field was applied to maximize the critical current with the same polarity as the bias current of the response measurement ($max\ I_c^+$). Having small values of differential resistance, the linewidth of the Josephson oscillation was small with the lowest value equals 97 MHz [11]. The calculated noise temperatures are higher than the physical temperatures, indicating excess noise (see Fig. 6).

VI. Discussion and Conclusion

Fig. 7 shows the normalized effective noise temperature T_{eff}/T versus W/λ_J. Differently shaped symbols are used for different junction types. The data points for the NKT sample are divided up into the two measurement regimes, $max\ I_c^+$,

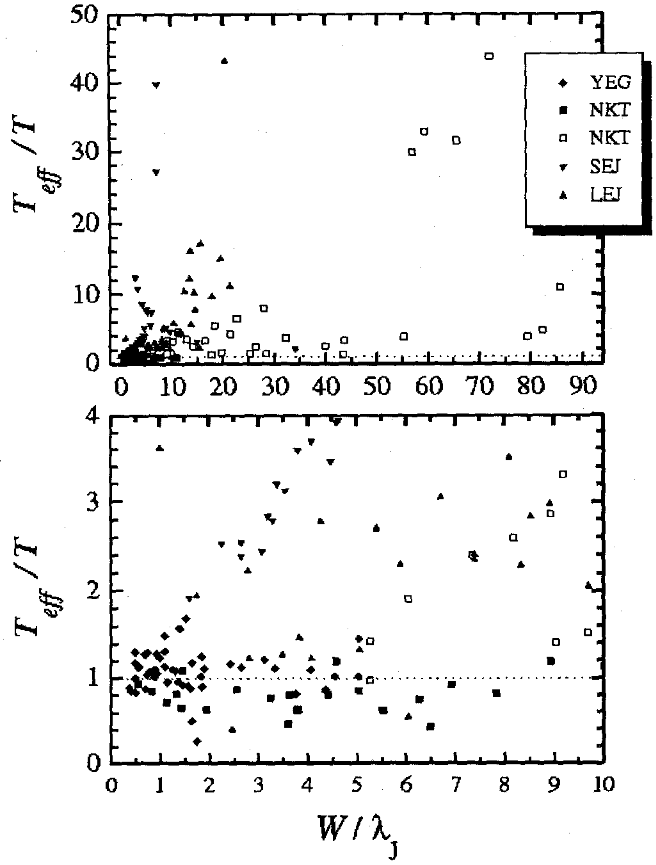

Figure 7. Noise temperature T_{eff}/T versus width W/λ_J for all junctions. Full symbols show data points obtained with an applied magnetic field to maximize the critical current with bias polarity, $max\ I_c^+$, open symbols for opposite bias polarity, $max\ I_c^-$. The lower graph shows an enlargement of the plot for $W/\lambda_J < 10$ and $T_{eff}/T < 4$.

(closed symbols), and $max\ I_c^-$ (open symbols). The bicrystal junctions data (NKT and Y-EG) are approximately equal to unity for the case $max\ I_c^+$. Maximizing the critical current with opposite polarity, ($max\ I_c^-$), the NKT data points (open symbols) show an elevated noise temperature for widths $W > 4\lambda_J$ The other junction types show increased noise temperatures already for smaller widths. This is probably due to the intrinsic inhomogeneous current distribution caused by the microstructure of the latter junctions.

Acknowledgment

The authors thank R. Gross and Yu. Ya. Divin for stimulating discussions. Provision of samples by A. Beck and R. Gross, University of Tübingen, Y. Shen, P. Vase and F. Freltoft from NKT Research Center, K. Herrmann, M. Siegel and A. Braginski, Forschungszentrum Jülich and R. Laibowitz, IBM Yorktown Heights is gratefully acknowledged.

References

[1] A. N. Vystavkin, V. N. Gubankov, L. S. Kuzmin, K. K. Likharev, V. V. Migulin, and V. K. Semenov, "S-c-S junctions as nonlinear elements of microwave receiving devices," *Rev. Appl. Phys.*, vol. 9, p. 79, 1974.

[2] Yu. Ya. Divin, O. Y. Polyanskii, and A. Y. Shulman, "Incoherent radiation spectroscopy based on the ac Josephson effect," *IEEE Trans. Mag.* **MAG**, vol. 19, no. 3 p. 613, 1983.

[3] Yu. Ya. Divin, J. Mygind, N. F. Pedersen, and P. Chaudhari, "Linewidth of Josephson oscillations in YBCO grain-boundary junctions," *IEEE Trans Appl. Supercond.* **AS**, vol. 3, p. 2337, 1993.

[4] G. M. Fischer, *High frequency properties of high temperature superconducting Josephson junctions.* Dissertation, University of Tübingen, 1996, Shaker Verlag, Aachen, Germany.

[5] G. M. Fischer, A. V. Andreev, Y. Y. Divin, J. Mygind, N. F. Pedersen, T. Freltoft, Y. Shen, and P. Vase, "ac Josephson effect in YBCO grain boundary junctions," *Physica B*, vol. 194, p. 1687, 1994.

[6] A. Beck, A. Stenzel, O. M. Froehlich, R. Gerber, R. Gerdemann, L. Alff, B. Mayer, and R. Gross, "Fabrication and superconducting transport properties of bicrystal grain boundary Josephson junctions on different substrates," *IEEE Trans Appl. Supercond.* **AS**, vol. 5, p. 2192, 1995.

[7] Yu. Ya. Divin, A. V. Andreev, G. M. Fischer, J. Mygind, N. F. Pedersen, K. Herrmann, V. N. Glyantsev, M. Siegel, and A. I. Braginski, "Millimeterwave response and linewidth of Josephson oscillations in YBCO step edge junctions," *Appl. Phys. Lett.*, vol.62, p1295, 1993.

[8] R. B. Laibowitz, R. P. Robertazzi, R. H. Koch, A. Kleinsasser, J. R. Kirtley, J. M. Viggiano, R. L. Sandstrom, and W. J. Gallagher. "Tunneling in all high Tc edge junctions with deposited barriers," *Phys. Rev. B*, vol. 46, p. 14830, 1992.

[9] G. M. Fischer, B. Mayer, H. Schulze, and R. Gross, " Critical current density distribution and magnetic flux states in YBCO grain boundary junctions," *IEEE Trans. Appl. Supercond.* **AS**, vol. 5, p. 2184, 1995.

[10] B. Mayer, H. Schulze, G. M. Fischer, and R. Gross, "Nonlocal response of grain-boundary type Josephson junction to local perturbation," *Phys. Rev. B*, vol. 52, p. 7727, 1995.

[11] G. M. Fischer, J. Mygind, N. F. Pedersen, and R. B. Laibowitz, "Linewidth measurements in YBCO edge junctions," in *ISEC'93 Extended Abstracts*, (Boulder, CO, USA), p. 225, 1993.